

High thermal stability of zero-field ferromagnetic resonance above 5GHz in ferrite-doped CoFe thin films

Guozhi Chai, Nguyen N. Phuoc, and C. K. Ong

Citation: *Appl. Phys. Lett.* **103**, 042412 (2013); doi: 10.1063/1.4816754

View online: <http://dx.doi.org/10.1063/1.4816754>

View Table of Contents: <http://apl.aip.org/resource/1/APPLAB/v103/i4>

Published by the [AIP Publishing LLC](#).

Additional information on *Appl. Phys. Lett.*

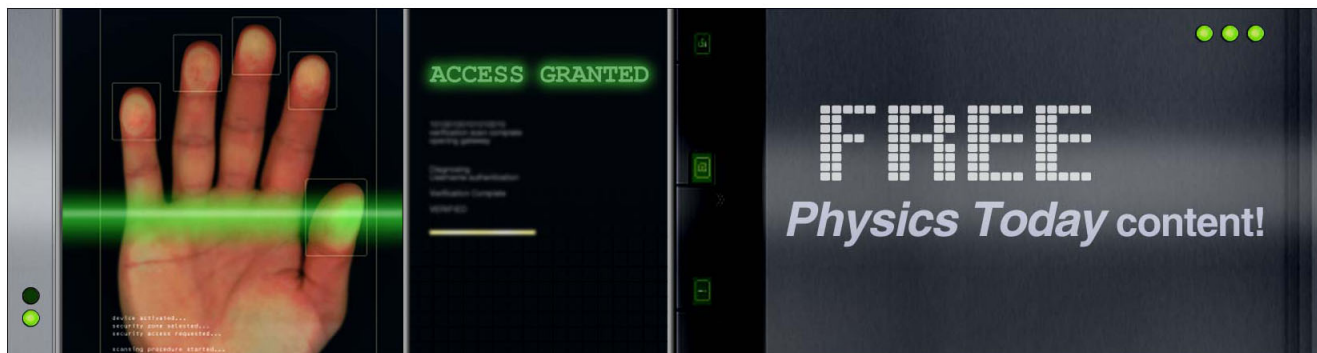
Journal Homepage: <http://apl.aip.org/>

Journal Information: http://apl.aip.org/about/about_the_journal

Top downloads: http://apl.aip.org/features/most_downloaded

Information for Authors: <http://apl.aip.org/authors>

ADVERTISEMENT



High thermal stability of zero-field ferromagnetic resonance above 5 GHz in ferrite-doped CoFe thin films

Guozhi Chai,^{1,a)} Nguyen N. Phuoc,¹ and C. K. Ong²

¹*Temasek Laboratories, National University of Singapore, Singapore 117411*

²*Department of Physics, Center for Superconducting and Magnetic Materials, National University of Singapore, Singapore 117542*

(Received 30 May 2013; accepted 10 July 2013; published online 24 July 2013)

Ferrite doped CoFe films with stripe domains are demonstrated to possess zero-field ferromagnetic resonance frequency above 5 GHz. The high resonance frequency is driven by the rotatable magnetic anisotropy propagated from the stripe domain structure and exchange coupling between rotatable ferrimagnetic spins and the ferromagnetic grains. The high temperature results show that these films have excellent thermal stability, which may have a great implication for microwave applications. © 2013 AIP Publishing LLC. [<http://dx.doi.org/10.1063/1.4816754>]

Soft magnetic thin films have been extensively utilized in many high frequency applications such as microwave noise filters, thin film inductors, and so on.^{1–5} As the operating frequency in many modern devices reaches towards gigahertz range, it is indispensable to seek magnetic thin films that possess a resonance frequency f_r higher than 5 GHz.⁶ Moreover, since many of such applications need to operate in environments where the temperature fluctuates drastically in a temperature range from 300 K to 420 K, it is required that the microwave properties of the magnetic thin films have a good thermal stability at least in this range.⁷ While the requirement for high f_r beyond 5 GHz can be fulfilled through the usage of exchange bias coupling between ferromagnet (FM) and antiferromagnet (AF),⁸ oblique deposition technique,⁹ or gradient composition deposition,^{10,11} it is quite difficult to realize a thin film that have good thermal stability with such a high f_r .^{12–14} The reason for this technical difficulty is mostly due to the substantial reduction of both magnetization and magnetic anisotropy (MA) with temperature when the films are heated up.^{12–14} In the present work, we demonstrate that this thermal stability problem can be resolved by employing rotatable magnetic anisotropy (RMA) to push the f_r towards a higher range, rather than traditionally using other kinds of MA such as unidirectional anisotropy or uniaxial anisotropy, which are more vulnerable to temperature changes. RMA was discovered many years ago mainly in two kinds of magnetic thin films: FM-AF exchange-biased systems^{15–18} and thin films with stripe domains.^{19–21} Very recently, RMA has also been found in ferrite doped FM thin films without stripe domain, which is in principle quite similar to the FM-AF exchange-biased system and may thus be placed into the first category.²² Here, we employ the RMA arising from both stripe domain structures and such a ferrite doped FM system to yield high f_r and good thermal stability in magnetic thin films. Since the stripe domain was found in magnetic thin films with thicknesses higher than a critical one, normally around 150 nm.^{19,20} The stripe domain structures were obtained by increasing the

thickness of the ferrite doped FM thin film to 180 nm, from our previous work of 110 nm.²²

The radio frequency (rf) magnetron sputtering chamber is used to deposit 180 nm thick ferrite doped CoFe magnetic thin films at ambient temperature onto 5 mm × 10 mm × 0.50 mm Si(100) substrates with background pressure lower than 5×10^{-7} Torr. The 3-inch Co₅₀Fe₅₀ targets have varying numbers of equal-sized 3 mm × 3 mm Ni_{0.5}Zn_{0.5}Fe₂O₄ ferrite chips attached. The compositions of the magnetic thin films were controlled by changing the number of Ni_{0.5}Zn_{0.5}Fe₂O₄ ferrite chips. During sputtering, an Ar flow rate of 16 SCCM (SCCM denotes cubic centimeter per minute at STP) was needed to maintain an Ar pressure of 2×10^{-3} Torr, and the rf power density was 2.7 W/cm². The thickness of the thin film was controlled both by the deposition time and by keeping the deposition rate constant, which was verified by a thickness profile meter. The composition of the films was determined by energy dispersive X-ray spectroscopy (EDS). Thicknesses of the thin films were measured by cross section image achieved by the SEM. The crystalline structure was characterized by grazing incidence X-ray diffraction (GIXRD, Panalytical Empyrean with Cu K α radiation). The surface image and magnetic domain state of the ferrite doped CoFe magnetic thin films are measured by Atomic Force Microscopy (AFM)/Magnetic Force Microscopy (MFM). The M_s and M-H loops were obtained by the vibrating sample magnetometer (VSM) with temperature range from 300 to 420 K. Permeability spectra were carried out with a vector network analyzer using the room temperature shorted microstrip transmission line³¹ and near field microwave microscope (NFMM) method from 500 MHz to 10 GHz with temperature range from 300 to 420 K.³² The temperature is meticulously controlled by changing the current applied to the heater and a thermocouple sensor attached to the sample holder to monitor the temperature.³² The angular dependence results of high frequency properties were measured with the NFMM by attaching the thin films onto an angular-resolved sample holder.

In this work we deposited ferrite doped CoFe thin films with thickness about 180 nm onto Si (100) substrates to obtain the stripe domain structures. By changing the ferrite chips on CoFe target, the composition of the different element Co, Fe, Ni, Zn can be found in Fig. 1(a). The

^{a)} Author to whom correspondence should be addressed. Electronic mail: tslcg@nus.edu.sg

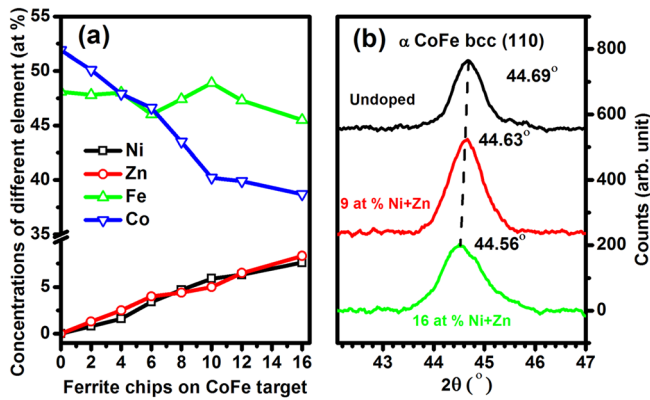


FIG. 1. (a) The composition of the thin film with different ferrite chips placed on the CoFe target. (b) The XRD spectrum shows peaks shift to the right as the doping concentration increases indicating grain sizes shrink as dopant elements increase.

concentration of Co reduces while Fe almost keeps constant with the dopant increasing, as Fe is also one element of the dopant. Ni and Zn increase linearly almost with the same ratio as the ratio in the source is also 1:1. Being concise, we use the concentration of Ni+Zn to indicate the concentration of dopant. Fig. 1(b) shows the XRD spectra of the film with different dopant concentration. It shows the diffraction peaks shift to the right as the doping concentration increases indicating grain sizes shrink as doping increases. The ferrite doped CoFe thin films have granular structures with CoFe grains surrounded by a matrix of amorphous Co-Fe-Ni-Zn-O oxide, only (110) peak of bcc structure CoFe grains can be found in the XRD results. As clear evidence shown in Figure 2 from AFM and MFM images for a representative CoFe film doped with 7% dopant, stripe domains are found in our films. The MFM image in Fig. 2(b) was taken with an arbitrary referenced direction for the film in remanent state, the typical domain width (bright or dark stripe) is about 85 nm. After that, a sufficiently large magnetic field of about 5 kOe was applied in the x-axis and reduced to zero so that the sample was in remanent state along the x-axis. Then the MFM

image was taken again as in Fig. 2(c) which unambiguously shows that the stripe domains are now aligned along the x-axis. A similar procedure was performed with the external applied field along the y-axis and the result was presented in Fig. 2(d) exhibiting a clear alignment of the stripe domains along the y-axis following the direction of the applied field. This observation clearly demonstrates that the direction of stripe domains can be rotated under a sufficiently large external magnetic field²¹ and this external field serves to define the RMA to be discussed later.

Two typical M-H loops of undoped and ferrite doped CoFe films are presented in Figures 3(a) and 3(b) together with the corresponding permeability spectra for each film in the insets. The hysteresis loops for undoped CoFe film exhibit normal magnetization curves without stripe domains and show no signature of the presence of in-plane anisotropy. This is also the case for all the films with dopant concentration less than 4%. However, when the dopant concentration reaches beyond 4% both easy axis and hard axis loops show superimposed curves with a specific shape characterized by a linear decrease of magnetization from its saturation value and a moderate remanence^{20,21} being a clear signature of the formation of stripe domains with the presence of out-of-plane magnetization component. The formation of stripe domain structures in those films (with dopant concentration higher than 4%) is also verified by MFM characterization as in Fig. 2. As the loops in both easy and hard axes are quite similar, one may expect that there is no significant static in-plane anisotropy in this case. However, the permeability spectra in the insets of Figs. 3(a) and 3(b) exhibit quite contradicting behaviors. For the film without doped ferrite as in the inset of Fig. 3(a), there is practically no visible peaks corresponding to ferromagnetic resonance FMR in the permeability spectra. This implies that the dynamic MA is not present in this case. Yet, for the films doped higher than 4% as in the inset of Fig. 3(b), a prominent peak at f_r around 6 GHz can be observed suggesting that there exists a large dynamic magnetic anisotropy field H_k^{dyn} even though the static magnetic anisotropy field H_k^{sta} in this case as shown in

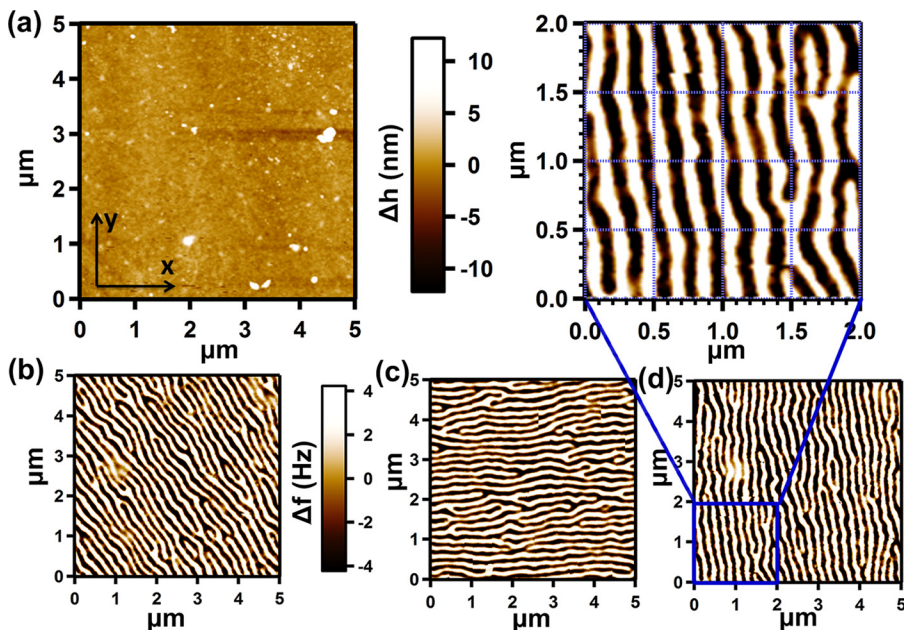


FIG. 2. (a) The surface image of the ferrite doped CoFe magnetic thin film taken by AFM. The color exhibits the roughness of the surface. (b) The MFM image taken for an as-deposited state in an arbitrary direction. The color represents the strength of the perpendicular component of spins. (c) MFM image in remanent state after the sample was placed under a sufficiently large field along the x-axis. (d) MFM image in remanent state after the sample was placed under a sufficiently large field along the y-axis. The image of higher magnification is also presented.

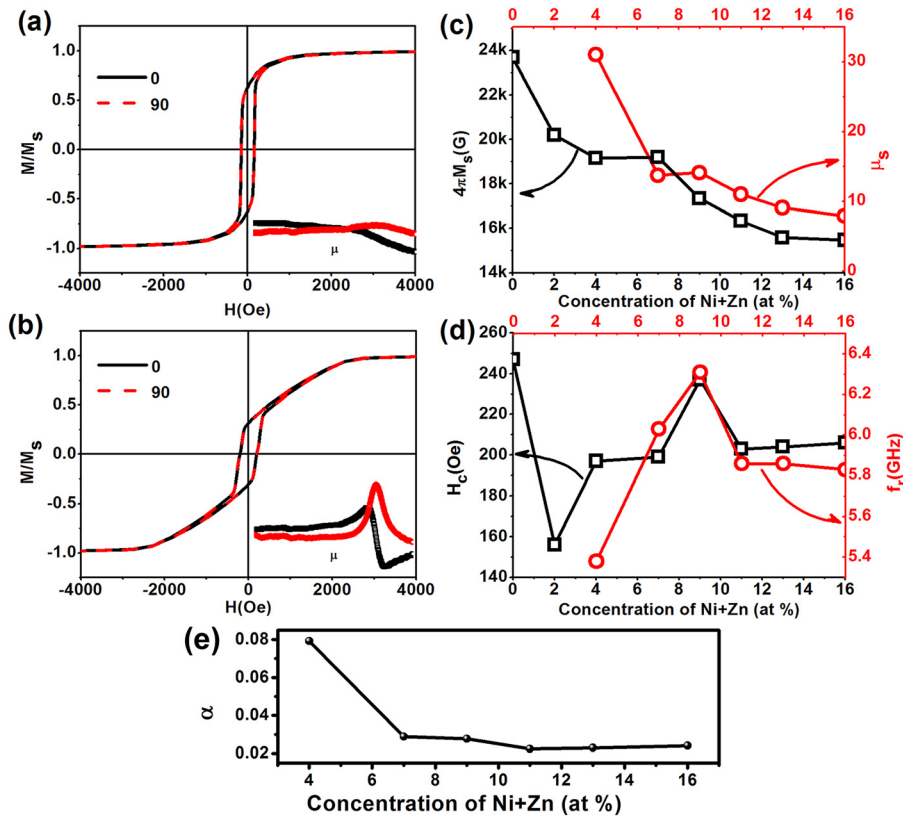


FIG. 3. The M-H loops of the (a) undoped and (b) ferrite doped CoFe magnetic thin films. The dark lines were taken at a random direction and the dashed red lines were taken at perpendicular direction of the initial direction. Insets show the high frequency permeability of the corresponding films. (c) The M_s (dark squares) and μ_s (red circles) depending on the concentration of the doped ferrite. (d) The H_c (dark squares) and f_r (red circles) as a function of the ferrite concentration. (e) The α as function of the ferrite concentration.

Fig. 3(b) is quite small. With the increasing of the doped ferrite concentration, the saturation magnetization M_s decrease from about 23.5 kG to 15 kG as shown in Fig. 3(c). The reason for this behavior is because the saturation magnetization of ferrite is much smaller than that of CoFe,^{22,23} thus causing a dilution of the magnetization of the ferrite doped CoFe films as observed. The static permeability μ_s estimated from the VSM is presented in Fig. 3(c) showing a similar decrease of μ_s with the increasing of ferrite dopant. This behavior can be easily understood as μ_s is proportional to M_s while it is inversely proportional with the H_k^{dyn} .^{17,18} H_k^{dyn} which is inclined to increase with the increasing of ferrite dopant.

The variation of coercivity H_c with the NiZn ferrite concentration is shown in Fig. 3(d). The H_c first decreases with ferrite concentration when the doped ferrite is less than 2%, then it is increased with further increase of dopant concentration up to 9%. The increase of the H_c may possibly be due to the emergence of the stripe domains.^{19,20} The H_c decreases when the dopant is increased from 9% to 16%. This behavior may be caused by the decrease of the grain size. According to random anisotropy model,^{24,25} the effective anisotropy fields H_k^{eff} in magnetic thin film increase as the separation of the grains increases. Thus, the H_k^{eff} and H_c increase when the ferrite concentration increases. Also presented in Fig. 3(d) is the variation of f_r with the concentration of doped ferrite. It is shown that f_r is increased from 5.4 GHz to 6.3 GHz when the dopant concentration is increased from 4% to 9%. This behavior can be understood within the framework of the emergence of the H_k^{dyn} , which is caused by the stripe domains and the ferrimagnetic spins. Once the stripe domains have been completely formed with dopant concentration reaching 9%, an increase in ferrite concentration does not lead to a further increase of the MA. The f_r is thus

slightly decreased down to 5.8 GHz because of the reduction of the saturation magnetization.

The damping coefficients α as function of doped ferrite concentration are shown in Fig. 3(e). It is interesting to observe that the damping factor is reduced to a very low level of around 0.02 with dopant concentration reaching 7%. This small value of α is very useful for high frequency applications. With the small damping value, the permeability spectra shown in the inset of Fig. 3(b) have an imaginary part being almost zero in the frequency range is lower than f_r indicating a very low magnetic residual loss in the films.²⁶

We argue that the presence of large H_k^{dyn} observed in the films with stripe domains in our case mostly stems from the contribution of H_k^{rot} . In order to verify this argument, we perform an investigation of the angular dependence of the high frequency permeability spectra^{22,27,28} with the result shown in Figure 4. The little variation of f_r measured at different orientations in Fig. 4(a) indicates that the high frequency responses of these films are isotropic. By fitting the

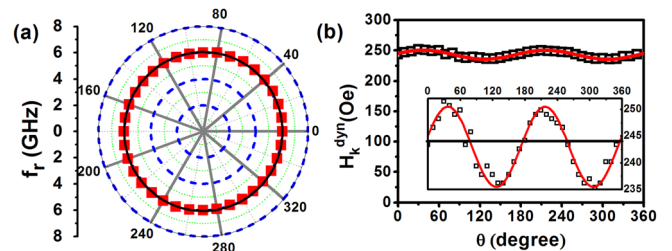


FIG. 4. (a) The angular dependence of the f_r for ferrite doped CoFe thin film without additional magnetic fields. (b) The dependence of H_k^{dyn} on θ for ferrite doped CoFe thin films. Inset shows the enlarged view of the result. The red line are the fitted curves to the equation $H_k^{\text{dyn}} = H_k^{\text{stat}} \cos 2\theta + H_k^{\text{rot}}$. The horizontal line is $H_k^{\text{rot}} = 243$ Oe.

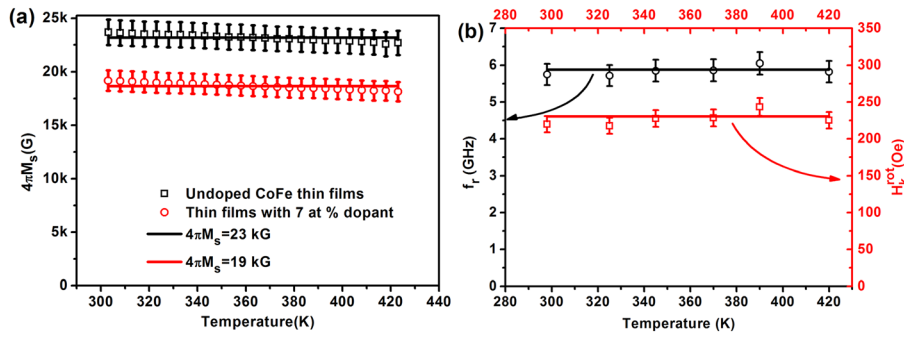


FIG. 5. (a) The $4\pi M_s$ - T curve of undoped CoFe magnetic thin films and with 7 at % dopant. (b) f_r and H_k^{rot} of CoFe magnetic thin films with 7 at % dopant as a function of temperature.

high frequency permeability spectra with LLG equation,²⁹ we can obtain the H_k^{dyn} of the magnetic thin films as shown in Fig. 4(b) as a function of the angle between the hard axis and RF excited field. This angular dependent experimental data of the H_k^{dyn} can be fitted to the following formula $H_k^{\text{dyn}} = H_k^{\text{rot}} + H_k^{\text{sta}} \cos 2\theta$.^{22,27} The first term is H_k^{rot} caused by the formation of rotatable stripe domains and can only sense by dynamics measurements^{17,18,22} while the second term is H_k^{sta} stemming from the static uniaxial anisotropy. The fitting results can be found in Fig. 4(b) with the inset of the figure showing an enlarged view of the fitting curve. From the fitting results, it is observed that the contribution from the static uniaxial anisotropy of about 8 Oe is much smaller than that of the H_k^{rot} which is 243 Oe. As the ratio of $H_k^{\text{rot}}/H_k^{\text{sta}}$ is so large that the main dynamic properties are driven by the H_k^{rot} ,²² we may conclude that the doped ferrite grains scattering in the film provide pools of rotatable stripe domain and ferrimagnetic spins to enhance isotropic anisotropy and raise the f_r .

Figure 5 revealing that ferrite doped CoFe films possess an excellent thermal stability for f_r . The $4\pi M_s$ - T curve shown in Fig. 5(a) suggests that for both pure CoFe films and ferrite doped CoFe films $4\pi M_s$ is slightly decreased less than 5% when the temperature is raised from 300 K to 420 K. It is noticed that the typical shape of M-H loops for thin films with stripe domains is still retained even when the temperature is increased up to 420 K. Previous studies of thermal stability of dynamic magnetization in several systems such as exchange bias system,^{13,30} or oblique deposition system,¹⁴ revealed that thermal stability of the f_r is rather poor especially for the case of f_r beyond 5 GHz, normally reduced at least 15% when the temperature is heated up from 300 K to 420 K.¹⁴ The reason for this significant reduction is due to the fall-off of MA with the increasing of temperature.^{12-14,30} However, in our case with ferrite doped CoFe films, the f_r is quite stable at about 6 GHz with temperature varied less than 5% as shown in Fig. 5(b). This result has a great implication from the application point of view as the requirement for thermal stability of high-frequency properties is crucially important for many microwave applications. Besides, from the fundamental perspective, this excellent thermal stability of ferrite doped CoFe films presents a challenge for the understanding of this intriguing behavior. As the mechanism for the emergence of the ultra-high f_r in our ferrite doped CoFe films is due to RMA, we may tentatively ascribe this RMA to the physical origin of the good thermal behavior of these films. The temperature dependence of H_k^{rot} in Fig. 5(b) exhibiting a stable behavior is supportive for our argument.

The H_k^{rot} in stems from the formation of stripe domains as well as the exchange coupling between the rotatable ferromagnetic spin and ferromagnetic spins. As aforementioned, the typical loop shape which is a signature of stripe domains is rather stable with temperature in our films, thus leading to the good thermal stability of the contribution of H_k^{rot} originated from stripe domains. For exchange coupling driven RMA, it is stable with the temperature especially for thin film thicker than 80 nm, which can also be found in AF/FM multilayers of our previous work³⁰ and we interpreted this stability in terms of the balance between the formed and the disappearing rotatable spins.³⁰ However, further study with more supporting evidence is still needed to verify this argument.

In summary, we report a type of ferrite doped CoFe magnetic thin films with ultra-high omnidirectional f_r and excellent thermal stability driven by RMA. The H_k^{rot} in this system originates from two different mechanisms leading to its very large value: one is due to the exchange coupling between rotatable ferrimagnetic spins and the ferromagnetic grains and the other one is due to the formation of stripe domain structures. Our finding of this kind of material suggests a route to tailor the high frequency properties of magnetic thin films with very good thermal stability to be used in high-frequency applications.

The financial support from the Defence Research and Technology Office (DRTech) of Singapore is gratefully acknowledged.

- ¹Y. W. Zhao, X. K. Zhang, and J. Q. Xiao, *Adv. Mater.* **17**, 915 (2005).
- ²S. A. Ramakrishna, *Rep. Prog. Phys.* **68**, 449 (2005).
- ³R. C. Che, L. M. Peng, X. F. Duan, Q. Chen, and X. L. Liang, *Adv. Mater.* **16**, 401 (2004).
- ⁴S. X. Wang, N. X. Sun, M. Yamaguchi, and S. Yabukami, *Nature* **407**, 150 (2000).
- ⁵G. Z. Chai, Y. C. Yang, J. Y. Zhu, M. Lin, W. B. Sui, D. W. Guo, X. L. Li, and D. S. Xue, *Appl. Phys. Lett.* **96**, 012505 (2010).
- ⁶K. Ikeda, K. Kobayashi, K. Ohta, R. Kondo, T. Suzuki, and M. Fujimoto, *IEEE Trans. Magn.* **39**, 3057 (2003).
- ⁷N. N. Phuoc and C. K. Ong, *Adv. Mater.* **25**, 980 (2013).
- ⁸N. N. Phuoc, F. Xu, and C. K. Ong, *Appl. Phys. Lett.* **94**, 092505 (2009).
- ⁹X. L. Fan, D. S. Xue, M. Lin, Z. M. Zhang, D. W. Guo, C. J. Jiang, and J. Q. Wei, *Appl. Phys. Lett.* **92**, 222505 (2008).
- ¹⁰S. Li, Z. Huang, J.-G. Duh, and M. Yamaguchi, *Appl. Phys. Lett.* **92**, 092501 (2008).
- ¹¹N. N. Phuoc, L. T. Hung, and C. K. Ong, *J. Alloys Compd.* **509**, 4010 (2011).
- ¹²M. Ledieu, F. Schoenstein, J.-H. Le Gallou, O. Valls, S. Queste, F. Duverger, and O. Acher, *J. Appl. Phys.* **93**, 7202 (2003).
- ¹³Y. Lamy, B. Viala, and I. L. Prejbeanu, *IEEE Trans. Magn.* **41**, 3517 (2005).

- ¹⁴N. N. Phuoc, G. Z. Chai, and C. K. Ong, *J. Appl. Phys.* **112**, 083925 (2012).
- ¹⁵M. D. Stiles and R. D. McMichael, *Phys. Rev. B* **59**, 3722 (1999).
- ¹⁶M. D. Stiles and R. D. McMichael, *Phys. Rev. B* **60**, 12950 (1999).
- ¹⁷J. McCord, R. Mattheis, and D. Elefant, *Phys. Rev. B* **70**, 094420 (2004).
- ¹⁸J. McCord, R. Kaltofen, T. Gemming, R. Huhne, and L. Schultz, *Phys. Rev. B* **75**, 134418 (2007).
- ¹⁹R. J. Prosen, J. O. Holmen, and B. E. Gran, *J. Appl. Phys.* **32**, 91S (1961).
- ²⁰J. B. Youssef, N. Vukadinovic, D. Billet, and M. Labrune, *Phys. Rev. B* **69**, 174402 (2004).
- ²¹G. X. Wang, C. H. Dong, W. X. Wang, Z. L. Wang, G. Z. Chai, C. J. Jiang, and D. S. Xue, *J. Appl. Phys.* **112**, 093907 (2012).
- ²²G. Z. Chai, N. N. Phuoc, and C. K. Ong, *Sci. Rep.* **2**, 832 (2012).
- ²³G. Z. Chai, D. W. Guo, X. L. Li, J. Y. Zhu, W. B. Sui, and D. S. Xue, *J. Phys. D* **42**, 205006 (2009).
- ²⁴G. Herzer, *IEEE Trans. Magn.* **26**, 1397 (1990).
- ²⁵D. S. Xue, G. Z. Chai, X. L. Li, and X. L. Fan, *J. Magn. Magn. Mater.* **320**, 1541 (2008).
- ²⁶J. B. Goodenough, *IEEE Trans. Magn.* **38**, 3398 (2002).
- ²⁷R. Lopusnik, J. P. Nibarger, T. J. Silva, and Z. Celinski, *Appl. Phys. Lett.* **83**, 96 (2003).
- ²⁸M. L. Schneider, A. B. Kos, and T. J. Silva, *Appl. Phys. Lett.* **86**, 202503 (2005).
- ²⁹T. L. Gilbert, *IEEE Trans. Magn.* **40**, 3443 (2004).
- ³⁰H. Y. Chen, N. N. Phuoc, and C. K. Ong, *J. Appl. Phys.* **112**, 053920 (2012).
- ³¹Y. Liu, L. F. Chen, C. Y. Tan, H. J. Liu, and C. K. Ong, *Rev. Sci. Instrum.* **76**, 063911 (2005).
- ³²L. T. Hung, N. N. Phuoc, X. C. Wang, and C. K. Ong, *Rev. Sci. Instrum.* **82**, 084701 (2011).